Supplemental Document

Optics Letters

Sub-diffraction-limit light sheet enabled by a super-oscillatory lens with an enlarged field of view and depth of focus: supplement

PEI HE,[1,2] WENLI LI,[1,2] CHENGXU AN,[1,2] XU SUN,[1,2,3] WEIZHENG YUAN,[1,2,4] AND YITING YU[1,2,5]

[1]*Research & Development Institute of Northwestern Polytechnical University in Shenzhen, Ningbo Institute of Northwestern Polytechnical University, School of Mechatronic Engineering, Northwestern Polytechnical University, Xi'an Shaanxi 710072, China*
[2]*Key Laboratory of Micro/Nano Systems for Aerospace (Ministry of Education), Key Laboratory of Micro and Nano-Electro-Mechanical Systems of Shaanxi Province, Northwestern Polytechnical University, Xi'an Shaanxi 710072, China*
[3]*e-mail: sunxu@nwpu.edu.cn*
[4]*e-mail: yuanwz@nwpu.edu.cn*
[5]*e-mail: yyt@nwpu.edu.cn*

Supplement DOI: https://doi.org/10.6084/m9.figshare.20032697

Parent Article DOI: https://doi.org/10.1364/OL.461730

Sub-diffraction-limit light sheet enabled by super-oscillatory lens with enlarged field of view and depth of focus: supplemental document

PEI HE,[1,2] WENLI LI,[1,2] CHENGXU AN,[1,2] XU SUN,[1,2,*] WEIZHENG YUAN,[1,2,*] AND YITING YU[1,2,*]

[1]*Research & Development Institute of Northwestern Polytechnical University in Shenzhen, School of Mechatronic Engineering, Ningbo Institute of Northwestern Polytechnical University, Northwestern Polytechnical University, Xi'an Shaanxi 710072, China*

[2]*Key Laboratory of Micro/Nano Systems for Aerospace (Ministry of Education), Key Laboratory of Micro and Nano-Electro-Mechanical Systems of Shaanxi Province, Northwestern Polytechnical University, Xi'an Shaanxi 710072, China*

*Corresponding author: sunxu@nwpu.edu.cn; yuanwz@nwpu.edu.cn; yyt@nwpu.edu.cn

---

S1. Multi-objective optimization of SOLs with enlarged field of view and depth of focus based on genetic algorithm

First, the I_i (i=1, 2, 3, 4, 5) is normalized, respectively, and the fitness function is established as shown in Eq. S1-1. The optimization process of genetic algorithm for SOLs to generate light sheets with sub-diffraction-limit thickness and reduced divergence simultaneously is shown in Fig. S1-1. The first step is to randomly create an initial population with 500 individuals. Then, the fitness function of each individual is calculated according to Eq. S1-1, by which the individuals are sorted and the lower ranked individuals are eliminated by elimination rate 0.2. The next generation is generated by gene recombination and mutation operation, and then the iteration begins. The maximum generation is 100 that defines the end of the iteration. The convergence time is about 32 hours in the case that the sampling interval is 0.9765nm and the Intel(R) Xeon(R) CPU E5-2620 v4 @ 2.10GHz (×2) are adopted.

$$Fit = I_1 + I_2 + I_3 + I_4 + I_5 \tag{S1-1}$$

$$I_1 = \sum_{i=1}^{N} I(\frac{(0.38+0.61)\lambda}{2NA}; f_i),\ ST = \frac{(0.38+0.61)\lambda}{2NA} \tag{S1-2}$$

where ST represents a coordinate on the x-axis between the super-oscillation standard and Rayleigh diffraction limit as shown in Fig. S1-2, at which the light intensity I is minimized by optimized iteration. By this way, focus size along x-axis of each discrete focus will be constrained between these two standards and the sidelobes can be well suppressed while breaking the diffraction limit.

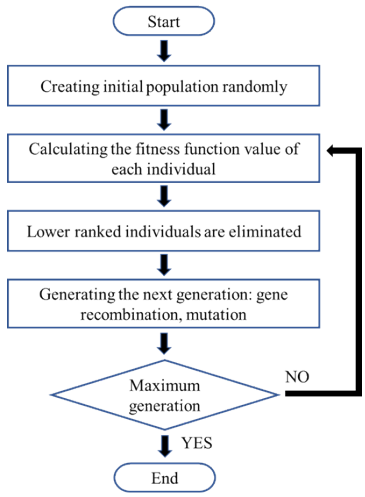

Fig. S1-1 Optimization procedure for SOLs to generate light sheets with sub-diffraction-limit thickness and reduced divergence, simultaneously.

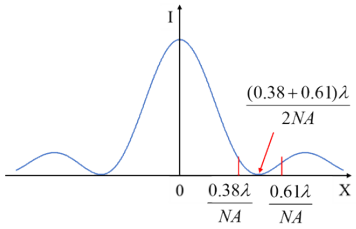

Fig. S1-2 Schematic diagram of optimizing focus size of each discrete focus.

S2. The wafer-level fabrication and optical measurement setup for light sheets generated by SOLs with enlarged field of view and depth of focus

The wafer-level fabrication flow for SOLs proposed in the manuscript is shown in Fig. S2-1. First, a layer of 100 nm Cr is deposited on the surface by electron beam evaporation. Then, a layer of 1 μm photoresist is covered onto the glass substrate by spin coating, followed by optical lithography. Finally, the Cr layer is patterned by ion beam etching and the arrays of SOL are obtained after photoresist removal. The every single SOL fabricated is with length (L) of 1000 μm and width (D) of 400 μm, as shown in Fig S2-2. The optical measurement setup for light sheets generated by SOLs is based on Nikon inverted microscope, as shown in Fig. S2-2. The 488 (±5) nm CW laser is adopted and its polarization direction parallel to the slits is defined by the polarizer. The TU plan fluor 50×/0.8 Nikon objective is fixed on piezoelectric scanning adapter ring (Physik Instrument, E-816) to scan the light field along the z-axis in steps of 100 nm, while working with the suitable high resolution camera (NIKON, 2560×1280) to capture every frame image. Finally the z-axis intensity distributions are formed by built-in data processing software ImageJ.

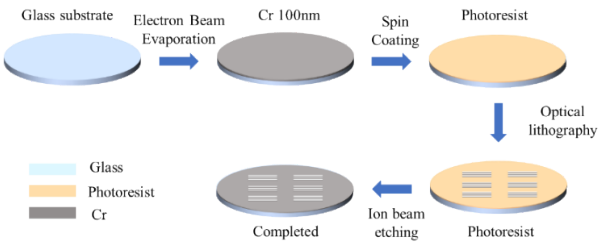

Fig. S2-1 Wafer-level fabrication flow of SOLs with enlarged field of view and depth of focus.

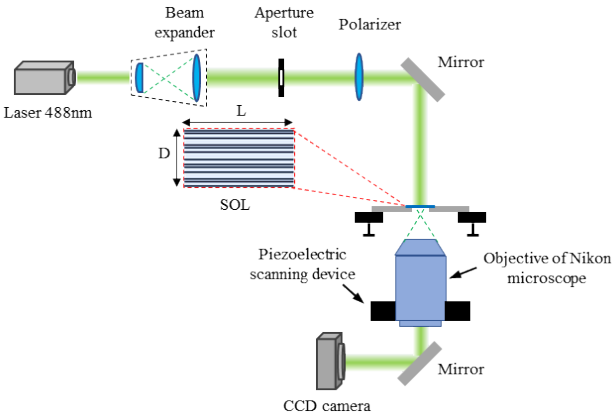

Fig. S2-2 Schematic of optical measurement setup for light sheets generated by SOLs with enlarged field of view and depth of focus.

S3. Focusing efficiencies of SOLs

The efficiencies of SOL#1, SOL#2, and SOL#3 mentioned in manuscript are 4.5%, 6.7% and 4.9% respectively, calculated theoretically by the ratio of total energy contained in the main lobe within the whole DOF to the total incident power.

S4. Intensity distribution in XY cross-section and three dimensional (3D) image

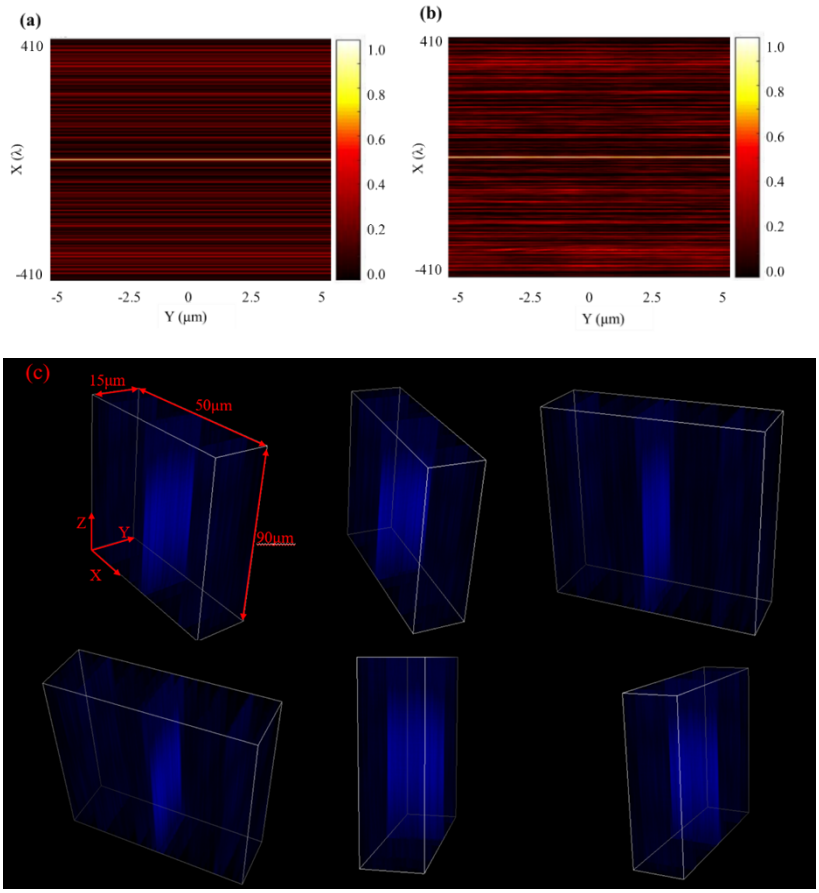

Fig. S4-1 Intensity distribution contours in XY cross-section: (a) theoretical and (b) experimental results of SOL #2 at the focal plane. (c) Three dimensional (3D) image of light sheet generated by SOL #2 captured in the experiment.